POTSDAM-INSTITUT FÜR KLIMAFOLGENFORSCHUNG

MODELLING PAST AND FUTURE LAND USE AND LAND COVER DYNAMICS IN THE NAKAMBE RIVER BASIN, WEST AFRICA

Gnibga Issoufou Yangouliba[1,3]*, Benewindé Jean-Bosco Zoungrana[2], Kwame Oppong Hackman[3], Hagen Koch[4], Stefan Liersch[4], Luc Ollivier Sintondji[5], Jean-Marie Dipama[2], Daniel Kwawuvi[1], Valentin Ouedraogo[6], Sadraki Yabré[1], Benjamin Bonkoungou[3], Madou Sougué[7], Aliou Gadiaga[6], Bérenger Koffi[8]

[1]Doctoral Research Program in Climate Change and Water Resources, National Water Institute, University of Abomey Calavi, P.O. Box 4521, Cotonou, Benin

[2]Department of Geography, Université Joseph Ki-Zerbo, 03 BP 7023, Ouagadougou, Burkina Faso

[3]West African Science Service Centre on Climate Change and Adapted Land Use (WASCAL), Competence Center, P.O Box 9507, Ouagadougou, Burkina Faso

[4]Potsdam Institute for Climate Impact Research (PIK), Member of the Leibniz Association, P.O. Box 60 12 03, 14412 Potsdam, Germany

[5]Department of Water for Agriculture and Society, National Water Institute, University of Abomey Calavi, P.O. Box 526, Cotonou, Benin

[6]WASCAL Climate Change and Human Habitat, Doctoral Research Programme, Federal University of Technology, PMB 65, Minna, Niger State, Nigeria

[7]Doctoral Research Program in Climate Change and Disaster Risk Management, University of Lomé, Lomé, Togo

[8]Laboratory of Science and Technology of Environment, Jean Lorougnon Guédé University, BP 150 Daloa, Côte d'Ivoire

***Corresponding author**: yangis2000@yahoo.fr; yangouliba.g@edu.wascal.org

Abstract

Understanding land use / land cover (LULC) dynamic is of great importance to sustainable development in Africa where deforestation is a common problem. This study aimed to assess the historical and future dynamics of LULC in the Nakambé River Basin. Landsat images were used to determine LULC dynamics for the years 1990, 2005 and 2020 using Random Forest classification system in Google Earth Engine while the predicted LULC of 2050 was simulated using the Markov Chain and Multi-Layer-Perceptron neural network in Land Change Modeler. The findings showed significant changes in LULC patterns. From 1990 to 2020, woodland and shrubland decreased by -45% and -68% respectively while water body, cropland and bare land/built-up increased by 233%, 51%, and 75%, correspondingly. From 2020 to 2050, the results revealed that under the Business-as-usual scenario, bare land/built-up and water bodies could continue to increase by 99% and 1% respectively. However, cropland, shrubland, and woodland could decrease by -32.61%, -33.91%, and -46.86%, respectively. Under the afforestation scenario, the contrary of Business-as-usual could occur. While woodland, shrubland, and cropland would increase by 22.24%, 51.57%, and 18.13%, correspondingly, between 2020 and 2050, the area covered by water bodies and bare land/built-up will decrease by -6.16% and -39.04%, respectively. The results of this research give an insight into past and future LULC dynamics in the Nakambé River Basin and suggest the need to strengthen the policies and actions for better land management in the region.

Keywords: Land Use/Land Cover, Random Forest, Markov Chain, Multi-Layer-Perceptron Neural Network, Land Change Modeler, Nakambé River Basin.

1. Introduction

LULC dynamics is described as a process of change of the Earth's land cover at temporal and spatial scales (Hassen et al. 2021). This change is increasingly becoming a global concern because of its impacts on terrestrial and aquatic ecosystems (Sibanda and Ahmed 2021). More than 75% of the Earth's already degraded land could reach 90% by 2050 (Cherlet et al. 2018). Between 1960 and 2019, almost one-third of the earth's land had changed (Winkler et al. 2021). These authors further emphasized a global net loss of forest area of 0.8 million km² but an expansion in global agriculture of 1.0 million km². However, these trends vary from one region to another. In Africa for instance, the natural vegetation of most places have been transformed to anthropogenic land uses (Barnieh et al. 2020; Bullock et al. 2021; Findell et al. 2017). Between 2012 and 2017, the continent's natural vegetation areas decreased significantly in favour of impervious areas (Nowak and Greenfield, 2020). This is due to population growth and the gradual drying up of soils due to climate change (PNUE 2004). In West Africa, between 1975 and 2013, large areas of savannah, open forest and woodland were converted to crop production and urban areas (Barnieh et al. 2020; CILSS 2016). Statistically, a third of the forest cover disappeared, while bare land areas increased by 47% over a period of 40 years (CILSS 2016).

From 1975 to 2013, the Mono River Basin for instance, saw an increase of 350% in farmland and decreases of -46% and -33% in woodland and shrubland, respectively (Koubodana et al. 2019). Additionally, these authors projected that between 2013 and 2027, agriculture would rise by 28% while woodland and shrubland would decrease by -10% and -21%, respectively. Many studies in the Volta Basin have also shown a changing trend from natural vegetation to cropland and built-up areas. For example, Braimoh and Vlek (2004) estimated 5% as the annual rate of natural vegetation conversion to cropland from 1984 to 1999 on an area of 5,400 km^2 located between the White Volta and Oti River Basins. Within the White Volta Basin, settlement increased by 46%, cropland increased by 49%, whereas forest and woodland decreased between 1990 and 2015 in the Nawuni sub-basin (Baatuuwie 2015). In the Bankandi-Loffing sub-basin, a part of the Black Volta Basin in Burkina Faso, a yearly conversion of 3.3% of savanna to cropland and settlement was observed between 2007 and 2013 (Idrissou et al. 2022, Yira et al. 2016). This rapid land use / land cover change (LULCC) is a major setback to sustainable development because it has negative impacts on agriculture, flood and drought occurrence, urban planning, as well as forest and water resource availability (Akinyemi, 2021; Akpoti et al. 2016; Bessah et al. 2020; Dimobe et al. 2017; Nut et al. 2021). Then, an assessment of LULCC could provide a better understanding of the interactions between natural vegetation and anthropogenic activities (Floreano and de Moraes 2021; Gupta and Sharma 2020).

The Nakambé River Basin (NRB) is part of the Sahel region where land degradation is a major issue (Forkuor et al. 2017). It occupies about 10% of the area of Burkina Faso and provides water to more than 6 million people for drinking, irrigation, livestock, and hydropower purposes. It contains nine protected areas of total area 1,301 km^2 which simply exist by virtue of their name because they are heavily degraded due to human activities (Belemsobgo et al. 2010). Moreover, many small dams have been built in the basin over the years. The Water Resources General Directorate (DGRE) reported more than 437 reservoirs in the basin (DGRE 2010). In addition, poor land management practices that do not protect the soil are reported in the basin (Nyamekye et al. 2018).

Several studies in the Upper NRB have highlighted an increase of bare land and cropland areas these last decades (Karambiri et al. 2011; Mahe et al. 2005; Yonaba et al. 2021). However, only a few studies have attempted to assess the dynamics of past and future LULC over the entire basin, which supports the hydrological processes of the largest reservoir, Bagre, in Burkina Faso, with particular emphasis on its annual water storage. Moreover, most of these studies used the maximum likelihood classification method. This method is based on the resemblance of neighbouring pixels. Despite its capability to provide acceptable results, the maximum likelihood classification method is parametric and assumes normal distribution of data (Shetty 2019). Nevertheless, several non-parametric machine learning algorithms that do not appeal to normal distribution have been developed and are also used in LULC assessment. These comprise mainly Random Forest (RF), Support Vector Machines (SVM), Classification and Regression Trees (CART), K-Nearest Neighbour (KNN), Learning Vector Quantization (LVQ), and Stochastic Gradient Boosting (SGB) (Dimobe et al. 2017; Forkuor et al. 2017; Gislason et al. 2006; Hackman et al. 2017; Nery et al. 2016; Shetty 2019; Zoungrana et al. 2015). Among these non-parametric classifiers, a consensus seems to have been reached on the effectiveness of RF.

Moreover, although various methods, such as the Cellular Automata-Markov Chain (CA-MC), Markov Chain Model (MCM), Stochastic Markov Chain (STMC), Multi-Layer Perceptron (MLP) Neural Network and Markov Chain Model, and Combined Markov-FLUS Model (Bozkaya et al. 2015; Dey et al. 2021; Girma et al. 2022; Sinha et al. 2020; Yang et al. 2022)have been developed to project future LULC, the most reliable technique is using the

Multi-Layer Perceptron Neural Network and Markov Chain Model, which is a robust machine learning algorithm for these projections (Eastman et al. 2020; Hussien et al. 2022) In this study, the RF algorithm helped to assess the historical dynamics of LULC, and the Multi-Layer Perceptron Neural Network and Markov Chain Model embedded in Land Change Modeler helped to predict the future LULCC in the NRB.

2. Materials and Methods

2.1. Study area

The Nakambé River basin is located in the Upper White Volta basin in Burkina Faso (Figure 1). It covers an area of about 32,623 km^2 at Niaogho discharge station. The basin is essentially spread over the South-Sahelian and North-Sudanese climatic zones (DGRE 2010) where annual rainfall ranges between 300 and 800 mm. The soils are dominated by tropical ferruginous leached soils and poorly evolved alluvial soils. These soils have low water retention capacities and are very sensitive to erosion. The landscape is dominated by agricultural lands although natural savannah areas still exist. The basin has been experiencing accelerated degradation since the 1970s (Thiombiano 2011). NRB encompasses several cities, including Ouagadougou, where about 3 million of the basin's 6 million people live (INSD 2020). The main economic activities remain agriculture and livestock. A multi-purpose dam (Bagré) was built to supply hydropower and water for irrigation (Figure 1).

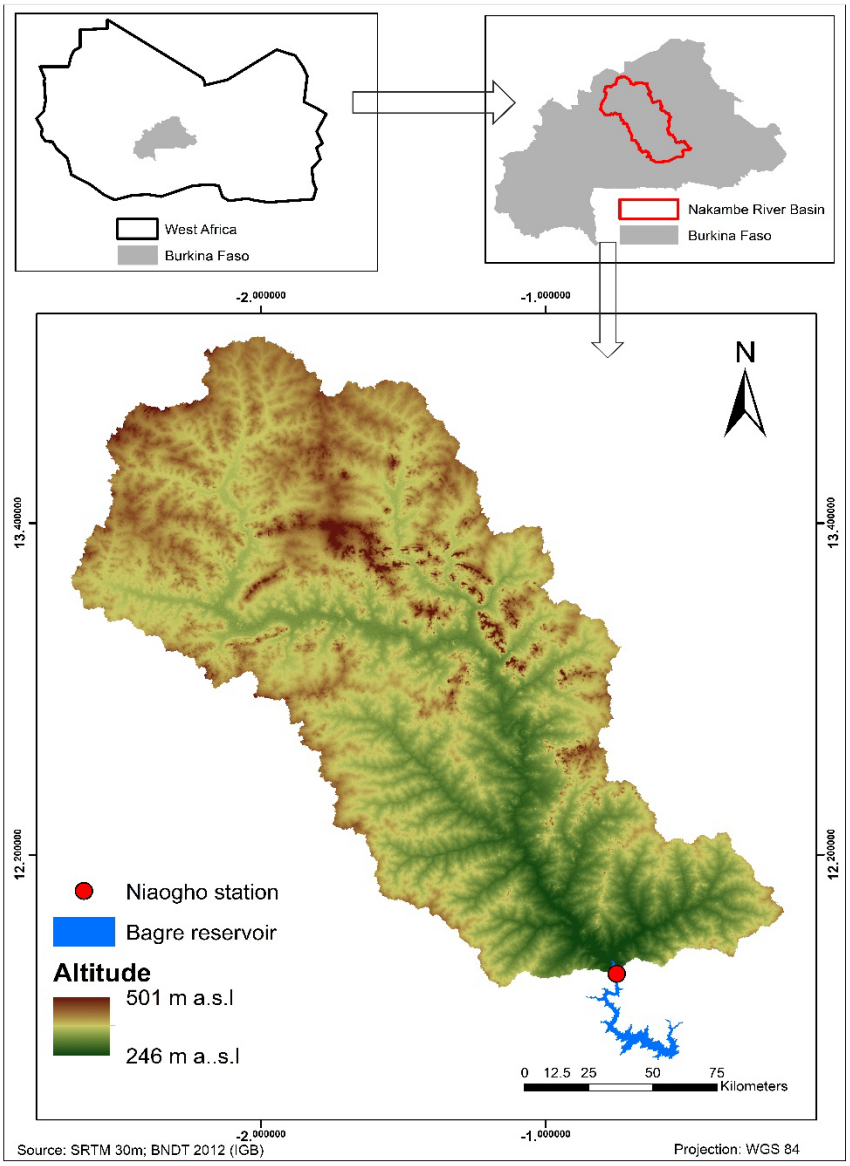

Figure 1. Map of the Nakambé River Basin in Burkina Faso

2.2. Data collection

The dataset used is composed of Landsat 5 TM images of the years1990 and 2005, and Landsat 8 OLI images of the year 2020. Landsat images have a spatial resolution of 30 meters and can be used to detect land use and land cover transition (Midekisa et al. 2017). For 1990 and 2020, Landsat 5 TM and Landsat 8 OLI surface reflectance image collections respectively from January 01 to December 31 were extracted from Google Earth Engine (GEE) Data Catalogue and used as inputs for the LULC analysis. To avoid having missing data due to the line scan corrector problem of Landsat 7, Landsat 5 TM was preferred for the year 2005. However, to obtain a cloud free image composite for the year 2005, the Landsat 5 TM surface reflectance images from 2003 to 2007 were used. This 2-year temporal window around 2005 was due to the low availability of Landsat 5 TM images covering the whole basin for the single year. Table 1 summarizes the scenes and bands of Landsat 5 TM and Landsat 8 OLI images used.

Table 1: Characteristics of Landsat satellite images used

Landsat images	Scenes	Selected bands	Spatial resolution	Temporal range
Landsat 5 (TM) Surface Reflectance	193052-53/194050-53/195050-53/196050-53	1,2,3,4,5,7	30m	01-01-1990 to 31-12-1990
Landsat 5 (TM) Surface Reflectance	193052-53/194050-53/195050-53/196050-53	1,2,3,4,5,7	30m	01-01-2003 to 31-12-2007
Landsat 8 (OLI) Surface Reflectance	193052-53/194050-53/195050-53/196050-53	2,3,4,5,6,7	30m	01-01-2020 to 31-12-2020

TM: Thematic Mapper, OLI: Operational Land Imager

Five main LULC classes were identified following a modified LULC classification scheme of Zoungrana et al. (2015). These are water body, woodland, shrubland, cropland, and bare land/built-up. Samples for each class were collected from three sources. The samples of the years 1990 and 2005 were collected using historical high-resolution images from Google Earth and land use and land cover databases from the National Geographic Institute of Burkina Faso, whereas a field survey was undertaken to collect samples for the year 2020. Overall, 992, 451, and 239 disproportional stratified random samples of the five LULC classes were used to classify the 1990, 2005, and 2020 images, respectively (Table 2).

Table 2. Sample sizes of LULC units for 1990, 2005, and 2020

LULC units	Sample sizes		
	1990	**2005**	**2020**
Water body	50	34	35
Woodland	170	52	30
Shrubland	346	84	32
Cropland	204	99	52
Bare land/built-up	222	182	90
Total	**992**	**451**	**239**

2.3. Data analysis

There are major issues that arise when analysing optical satellite data on large areas such as the NRB because they cover many scenes. These include data size management and availability cloud-free images (Floreano and de Moraes 2021). One of the most efficient ways to deal with these issues is to use cloud-based computational platforms such as GEE that provide scientists globally almost limitless opportunities for big data management and processing and allow easy integration of freely available remotely sensed images with other spatial data to tackle the complex socio-environmental issues of our time (Hackman et al. 2020). In other words, the GEE cloud-based platform is of great importance because it allows easy and fast analysis of data on large spatial regions using high-performance computing resources without the need to download them (Fattore et al. 2021). In addition, it provides computation tools to process large collections of satellite images over wide temporal ranges. For example, by using

different filters, it is possible to exclude certain images depending on the seasonality and cloud coverage. This is important for studies of areas in regions such as the West African region that lack atmospherically undisturbed and cloud free satellite images, mainly in the rainy season (Zoungrana et al. 2015).

2.3.1. Data pre-processing

The pre-processing steps involved scaling, cloud masking and additional bands computation. The scaling consisted of applying the respective scale factors and offsets to the images in order to get the true surface reflectance values. The cloud masking involved the identification of all pixels with the clouds and shadows to exclude them from further analysis. The median filter was then applied to the resulting images for each year to obtain a cloud free composite. In addition to the five raw surface reflectance bands, the Normalized Difference Vegetation Index (NDVI) and the Normalized Difference Built-up Index (NDBI) were computed and used as additional features. The NDVI allows to get a clear differentiation of vegetation from non-vegetation classes (Barnieh et al. 2020; Feng et al. 2016; Hackman et al. 2017; Yu et al. 2014) while NDBI allows to get a differentiation of built-up and bare land areas from other land uses (Hackman et al. 2020; Prasomsup et al. 2020).

2.3.2. Image classification and accuracy assessment

The pre-processed images were classified using the training samples mentioned in Table 2. For each year, 70% of samples were used to train the classification algorithm while 30% were utilized for testing. The method of classification was based on the RF supervised classification. As an ensemble classifier formed by the combination of multiple trees that is resistant to noise and overfitting issues, RF is able to process massive high-dimensional data while maintaining high accuracy (Gislason et al. 2006; Shetty 2019). It has been successfully used for LULC assessment in Burkina Faso by different researchers (Dimobe et al.2017; Zoungrana et al. 2015). Furthermore, it is reportedly the best classifier for soil (Forkuor et al. 2017) and LULC mapping (Hackman et al. 2017; Thiam et al. 2022) compared to SVM and SGB in Burkina Faso, Ghana and Togo, respectively. Thus, Nery et al. (2016) suggested that RF and SVM should be prioritised when classifying time series imagery for LULCC detection.

The classification accuracies were assessed through overall accuracy (OA), and Kappa index (K) following the Equations 1 and 2 described below by Rwanga and Ndambuki (2017).

$$OA = \frac{\sum_1^n x}{\sum_1^n X} \qquad (1)$$

where x is the number of correctly classified samples and X is the total of samples.

$$K = \frac{N\sum_{i=1}^{r} x_{ii} - \sum_{i=1}^{r}(x_i + Xx_{+1})}{N^2 - \sum_{i=1}^{r}(x_{ii} + Xx_{+1})} \qquad (2)$$

where r = number of rows and columns in error matrix, N = total number of observations (pixels), x_{ii} = observation in row i and column i, $Xi+$ = marginal total of row i, and $X+i$ = marginal total of column i.

Also, the confusion matrix for the LULC maps, 1990-2005, 2005-2020, and 1990-2020, was computed. The confusion matrix allows for knowing the sources of misclassification for a LULC unit (Liu et al. 2020).

2.3.3. LULCC analysis and spatial trend of anthropogenic land use

The dynamics between the different LULC classes were examined following the change analysis module of the Land Change Modeler. Moreover, percent change was computed following equation (3) (Hussien et al. 2022).

$$p = \frac{(A_l - A_e)}{A_e} \text{x } 100 \qquad (3)$$

where p is the percent change, A_l is the area of a class in the later LULC map (km^2), and A_e is the area of a class in the earlier LULC map (km^2).

The spatial trend of anthropogenic land use was assessed with the spatial trend tool of Land Change Modeler. It consists of mapping the conversion from one or multiple classes of LULC to another following a polynomial function. The study used a third-degree polynomial function to map the spatial trend (Eastman 2020).

2.3.4. Land use change driver variables and transition potentials mapping

Changes in land use result from multiple variables consisting of physical and human factors. Many variables are commonly used in LCM to explain the change in land use. These are composed of the slope, elevation, soil, distance to reservoirs, distance from rivers, distance from roads, distance to urban, etc. (Gharaibeh et al. 2020; Hussien et al. 2022; Kim et al. 2020; Larbi et al. 2019). In this study, four drivers namely, (i) distance to roads, (ii) distance to urban, (iii) distance to rivers, and (iv) evidence likelihood, were considered and used as inputs in the Transition Sub-Model Structure.

The major potential transitions from one LULC class to another were mapped using the MLP neural network algorithm (Larbi et al. 2019). According to Eastman (2020), MLP neural networks are the most robust technique for transition potential mapping, even though the logistic regression method is also viable. Moreover, it allows one to model several or even all transitions at once and is quite capable of modelling non-linear relationships (Eastman, 2020). In this study, nine major transitions greater than 100,000 hectares, derived from the change analysis were considered to model the potential transitions. These are shrubland to woodland; woodland to shrubland; cropland to shrubland; woodland to cropland; shrubland to cropland; bare land/built-up to cropland; shrubland to bare land/built-up; and cropland to bare land/built-up. After running the transition sub-model using an MLP neural network, the transition potential maps were successfully implemented. The output of the transition sub-model gives the model skill and the most and least influencing driver variables. According to Hussien et al. (2022) and Clark Labs (2020), a model that forces a single independent variable to be constant while keeping one variable constant at a time explains better the power of explanatory drivers than the Cramer's V method. Figure 2 summarizes the methodology used in this study.

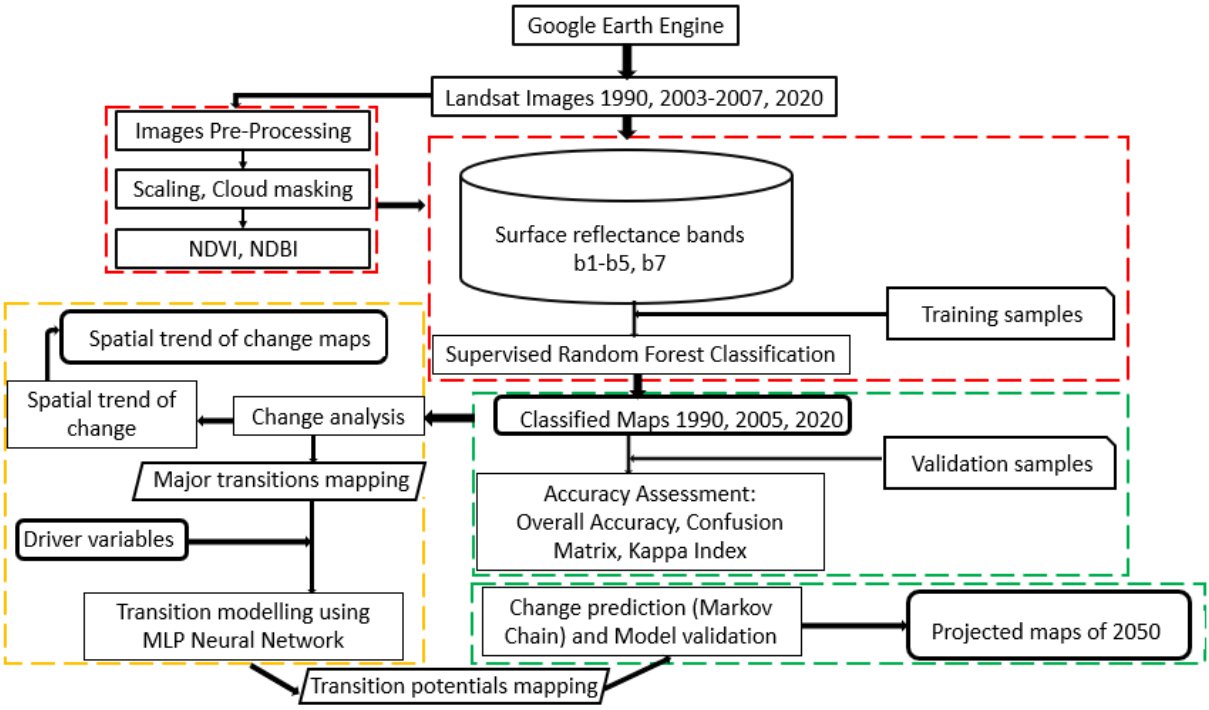

Figure 2. LULC mapping and modelling Flowchart

2.3.5. Model validation and LULCC projection

To simulate the LULC of 2020, the first period of 1990-2005 was considered. The simulation was done using the Markov Chain Model. This technique is described and used in several studies to project future LULC (Larbi et al. 2019; Mehrabi et al. 2019; Näschen et al. 2019; Shade and Kremer 2019; Koko et al. 2020). The simulated LULC map of 2020 was then compared to the actual LULC of 2020 for validation. This process used the module VALIDATE, which allows the computation of the Kappa index (Pontius 2000). The Kappa index ranges from -1 to 1 and shows the agreement or disagreement between the actual and simulated maps (Pointus 2000). After the model validation, the future LULC of 2050 was computed based on the same drivers and parameters, and changes

detected in LULC between 1990 and 2020. Two futures scenarios were adopted, which were included in the Markov Chain Model editing matrix to model the 2050 LULC. The Business-as-usual (BAU) scenario assumes a probability of decreasing natural vegetation (woodland and shrubland) to the benefit of cropland and bare land/built-up, and a decrease of cropland to the benefit of bare land/built-up. The afforestation scenario assumes a probability of increasing natural vegetation (shrubland + woodland) at the expense of cropland and a decrease in bare land/built-up to the benefit of cropland, as summarized in Table 3. The choices for these transitions in the scenarios are based on reasonable knowledge of the field.

Table 3. Probability of changes used for BAU and afforestation scenarios

BAU	AFFORESTATION
10% Woodland to cropland	5% Cropland to woodland
10% Woodland to bare land/built-up	5% Bare land/built-up to woodland
15% Shrubland to cropland	15% Cropland to shrubland
10% Shrubland to bare land/built-up	5% Bare land/built-up to Shrubland
30% Cropland to bare land/built-up	30% Bare land/built-up to cropland

3. Results

3.1. Accuracy of Land Use and Land Cover Classification

The results of the classification have an overall accuracy of 81%, 91%, and 93% while the Kappa coefficients are 91%, 82% and 76% for 1990, 2005 and 2020, respectively. Tables 4-6 show the statistics of the confusion matrix for the 1990, 2005 and 2020 LULC maps, respectively.

Table 4. Confusion matrix of the LULC classification in 1990

LULC 1990	Water body	Woodland	Shrubland	Cropland	Bare land/built-up
Water body	**100.0**	0.0	0.0	0.0	0.0
Woodland	0.0	**85.4**	14.6	0.0	0.0
Shrubland	0.0	5.2	**94.8**	0.0	0.0
Cropland	0.0	0.0	3.9	**94.1**	2.0
Bare land/built-up	0.0	0.0	0.0	2.0	**98.0**

Table 5. Confusion matrix of the LULC classification in 2005

LULC 2005	Water body	Woodland	Shrubland	Copland	Bare land/built-up
Water body	**100.0**	0.0	0.0	0.0	0.0
Woodland	0.0	**66.7**	33.3	0.0	0.0
Shrubland	0.0	14.3	**85.7**	0.0	0.0
Cropland	0.0	0.0	7.7	**76.9**	15.4
Bare land/built-up	0.0	0.0	0.0	2.7	**97.3**

Table 6. Confusion matrix of the LULC classification in 2020

LULC 2020	Water body	Woodland	Shrubland	Copland	Bare land/built-up
Water body	**100.0**	0.0	0.0	0.0	0.0
Woodland	0.0	**62.5**	37.5	0.0	0.0
Shrubland	0.0	0.0	**66.7**	33.3	0.0
Cropland	0.0	0.0	0.0	**87.5**	12.5
Bare land/built-up	0.0	0.0	0.0	20.0	**80.0**

3.2. Land Use and Land Cover maps in 1990, 2005, and 2020

The results of the LULC maps of 1990, 2005 and 2020 are shown in Figure 2 and Table 7. In 1990, the NRB was mainly covered by shrubland (44%) and cropland (36%). These were followed by bare land/built-up, woodland and water body with coverages of 16%, 3% and 0.5% respectively. However, in the year 2005 the order was reversed. Cropland and shrubland covered 49% and 29%, respectively. As in 1990, woodland and water body were the less represented LULC. In 2020, the basin's land cover was dominated by cropland (54%), followed by bare land/built-up (29%) and shrubland (14%). From 1990 to 2020, the natural vegetation has given place to anthropogenic land uses (cropland and bare land/built-up) (Figure 3).

Table 7. Proportion of LULC units in 1990, 2005 and 2020

LULC units	1990		2005		2020	
	km^2	%	km^2	%	km^2	%
Water body	131	0.40	202	0.62	436	1.34
Woodland	946	2.90	646	1.98	522	1.60
Shrubland	14,491	44.42	9,500	29.12	4,652	14.26
Cropland	11,739	35.98	15,950	48.89	17,691	54.23
Bare land/Built-up	5,316	16.30	6,326	19.39	9,322	28.57
Total	32,623	100	32,623	100	32,623	100

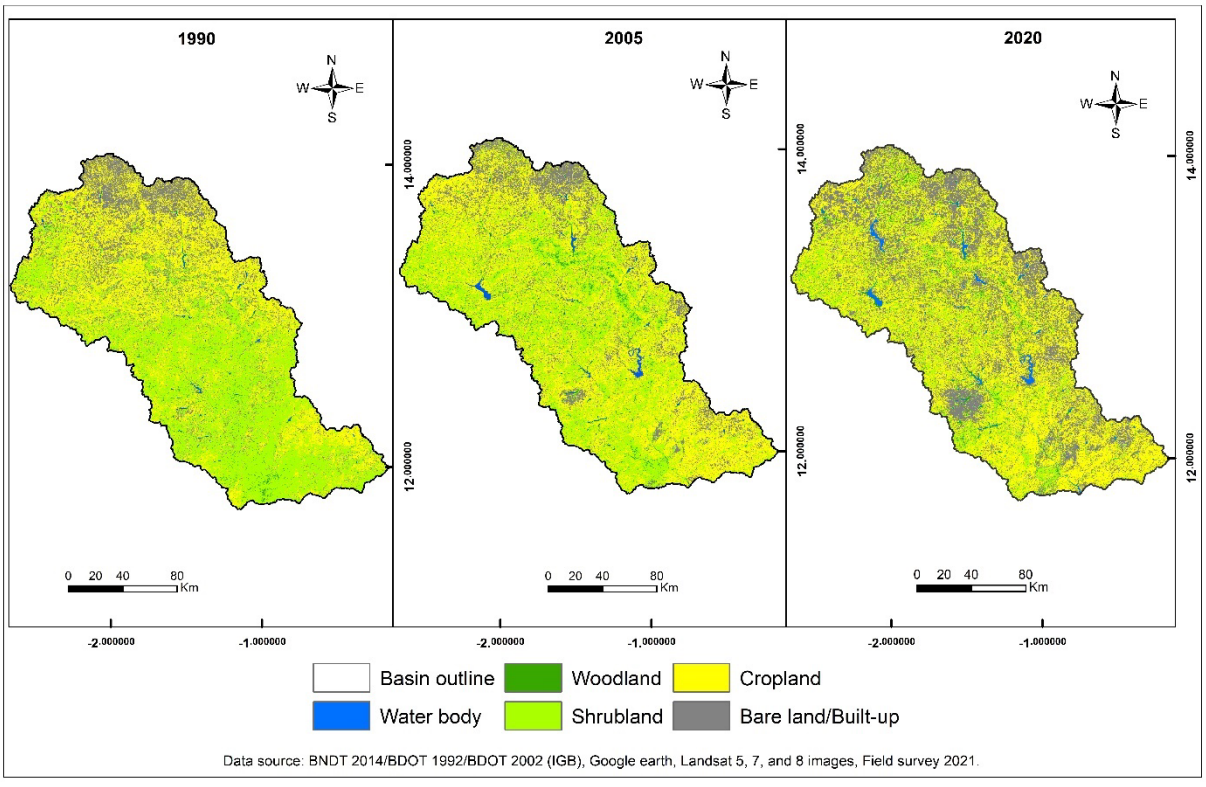

Figure 3: LULC maps of 1990, 2005, and 2020

3.3. Changes in Land Use and Land Cover between 1990-2005, 2005-2020, and 1990-2020

During 1990-2020, losses and gains were observed in LULC units. For the first fifteen years (1990-2005), the LULC classes that decreased were woodland (-32%) and shrubland (-34%), while water bodies, cropland, and bare land/built-up increased by 54%, 36%, and 19%, respectively (Figure 4). From 2005–2020, the same dynamics were noticed, with different percentages of change. Woodland and shrubland decreased by 19% and 51%, respectively, while an increase of 116%, 11%, and 47% were also observed for water bodies, cropland, and bare

land/built-up, correspondingly. The high increase in water bodies' area could be due to the construction of the Ziga and Dourou dams. Overall, during the last 31 years, the NRB experienced an increase in water bodies (233%), cropland (51%), and bare land/built-up (75%). These increases were likely at the expense of woodland and shrubland, which decreased by -45% and -68%, respectively, from 1990-2020 (Figure 3).

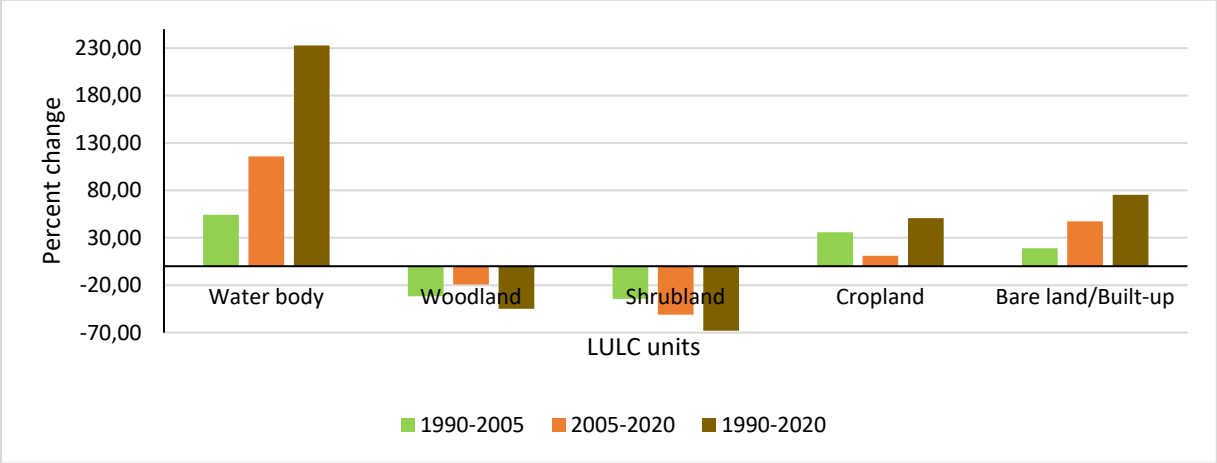

Figure 4. Percent of changes of LULC units between 1990-2005, 2005-2020, and 1990-2020

3.4. Contributors to cropland and bare land/built-up increase

The contributors to the increase in cropland and bare land/built-up are shown in Figure 4. During the period 1990-2005, the increase in cropland could mostly be attributed to the decrease in shrubland of 3,200 km^2 while the increase in bare land/built-up could be attributed to the decrease in cropland of 900 km^2. However, from 2005 to 2020 the decrease in shrubland of almost 4,000 km^2 were transformed to cropland, even though more than 3,000 km^2 of the existing cropland in 2005 had been transformed into bare land built-up in 2020. This is illustrated in Figure 5 as the gains in bare land/built-up between 2005 and 2020 are typically from cropland and shrubland, respectively. Overall, from 1990-2020, the increase in cropland could be attributed to the major loss of 6,000 km^2 of shrubland, representing 19% of the total area. Meanwhile, the increase in bare land/built-up from 2005-2020 could be attributed to the losses in cropland (2,000 km^2) and shrubland (1800 km^2) areas.

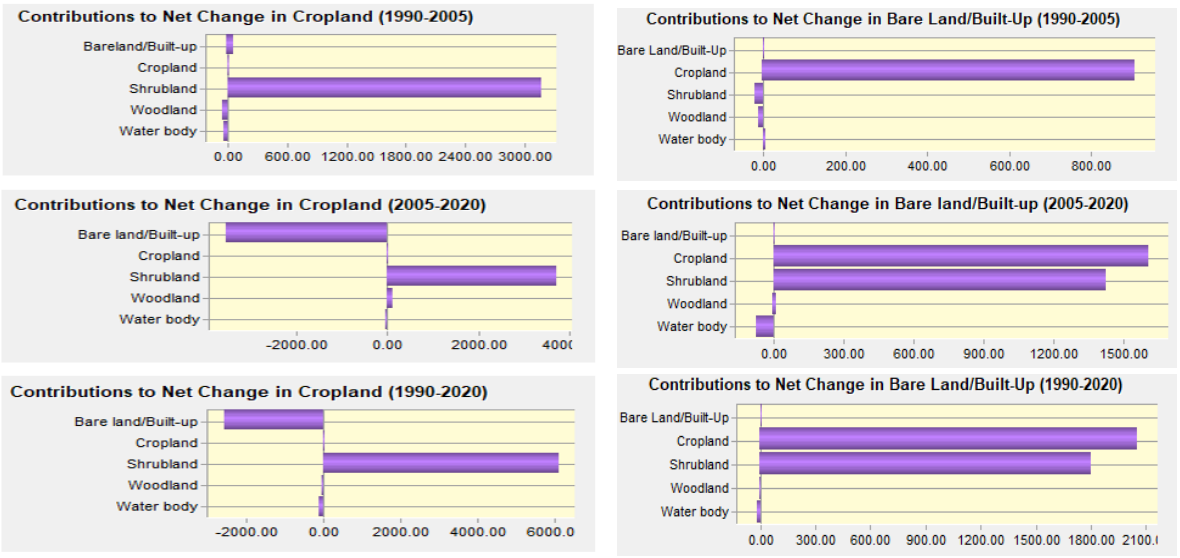

Figure 5. Contribution to net changes in cropland and bare land/built-up (in km^2) for 1990-2005, 2005-2020 and 1990-2020.

3.5. Spatial trend of anthropogenic land uses

The spatial trend of other land use conversions to cropland and bare land/built-up from 1990-2005 and 2005-2020 are shown in Figures 6 (cropland) and 7 (bare land/built-up), respectively. It can be observed that the

transformation of other LULC classes to cropland and bare land/built-up is South-Eastward from 1990-2005 while during the period 2005-2020, the conversion trend is North-Westward. Also, there was somewhat strong correlation between cropland and bare land/built-up classes. During the first fifteen years, the intensity of change was higher for cropland (0.4) than bare land/built-up (0.15) whereas from 2005 to 2020, the amplitude of change for cropland (0.24) and bare land/built-up (0.26) was quiet the same (Figures 6 and 7).

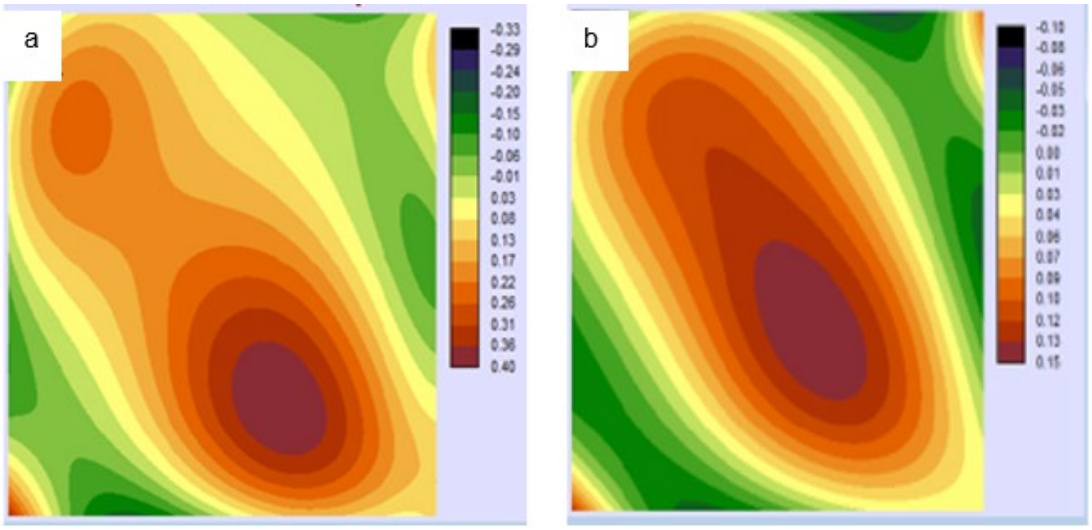

Figure 6. Spatial trend of conversion from all LULC classes to cropland (a) and bare land-built-up (b) during the period 1990-2005. Negative values represent a reverse spatial development for the analysed trend, whereas increasing positive values characterize an increasing intensity for the analysed trend.

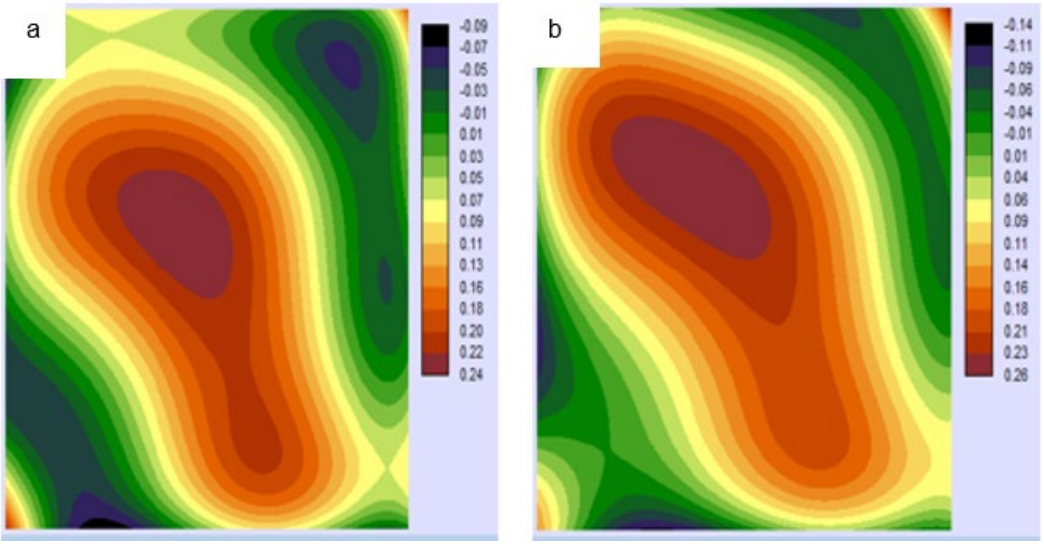

Figure 7. Spatial trend of conversion from all LULC classes to cropland (a) and bare land-built-up (b) during the period 2005-2020. Negative values represent a reverse spatial development for the analysed trend, whereas increasing positive values characterize an increasing intensity for the analysed trend.

3.6. Land use change driver variables and potential transition mapping

The four driver variables (Figure 8) were used to run the potential transition from one class to another. The model succeeded in creating the potential transition maps with an acceptable accuracy rate of 76% (Eastman, 2020). The results also highlight the relationship between the driver variables and land use change during the period 1990-2005. Indeed, the evidence likelihood was found to be the most influential variable (0.5) driving the land use change while the distance to rivers was found as least influential variable (0.23).

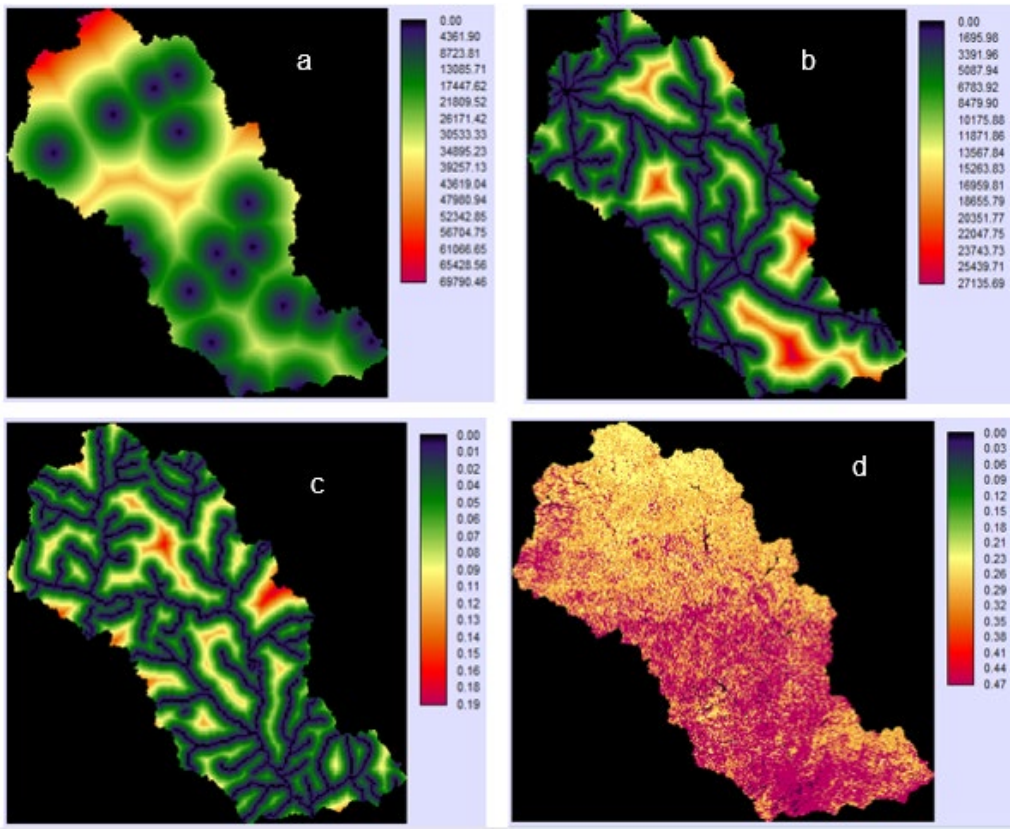

Figure 8. Explanatory variables used for the transition potential mapping (a) Distance to urban, (b) Distance to roads, (c) Distance to rivers, (d) Evidence Likelihood.

3.7. Model validation

The simulated and classified maps of 2020 were compared by using the VALIDATE module in Idrisi software. K_{no} evaluates the overall accuracy of the model while $K_{locality}$ indicates the model's ability to identify correct locations (Sibanda and Ahmed 2021). The results showed a K_{no} of 0.86 and a $K_{locality}$ of 0.85, indicating the model's ability to simulate the projected LULC of 2020 although there are some slight differences between the two maps of 2020 (Figure 9). The model tends to overestimate bare land/built-up, shrubland, and woodland areas while it underestimates water body and cropland areas (Table 8). For instance, the difference between the simulated and the classified bare land/built-up is 2,276 km^2, indicating an error of 24.42%. As for cropland, the area of the simulated map (14,936 km^2) is less than the classified map (15,950 km^2), showing an error of 5.71% (Table 8). The great difference between the simulated and classified water bodies' class could be due to the fact that the simulation was done with LULC maps (1990 and 2005) that existed before Tougou and Seguenega dams' construction.

Table 8. Proportion of classified and simulated LULC units in 2020 and their associated errors

LULC units	Classified 2020		Simulated 2020		Error (difference between Simulated 2020 and classified 2020)	
	km^2	%	km^2	%	km^2	% Change
Water body	436	1.34	235	0.72	-201	46.10
Woodland	522	1.6	660	2.33	138	26.44
Shrubland	4652	14.26	5091	15.6	439	9.44
Cropland	15950	48.89	15039	45.79	-911	5.71
Bare land/ Built-up	9322	28.57	11598	35.55	2276	24.42
Total	32623	100	32623	100		

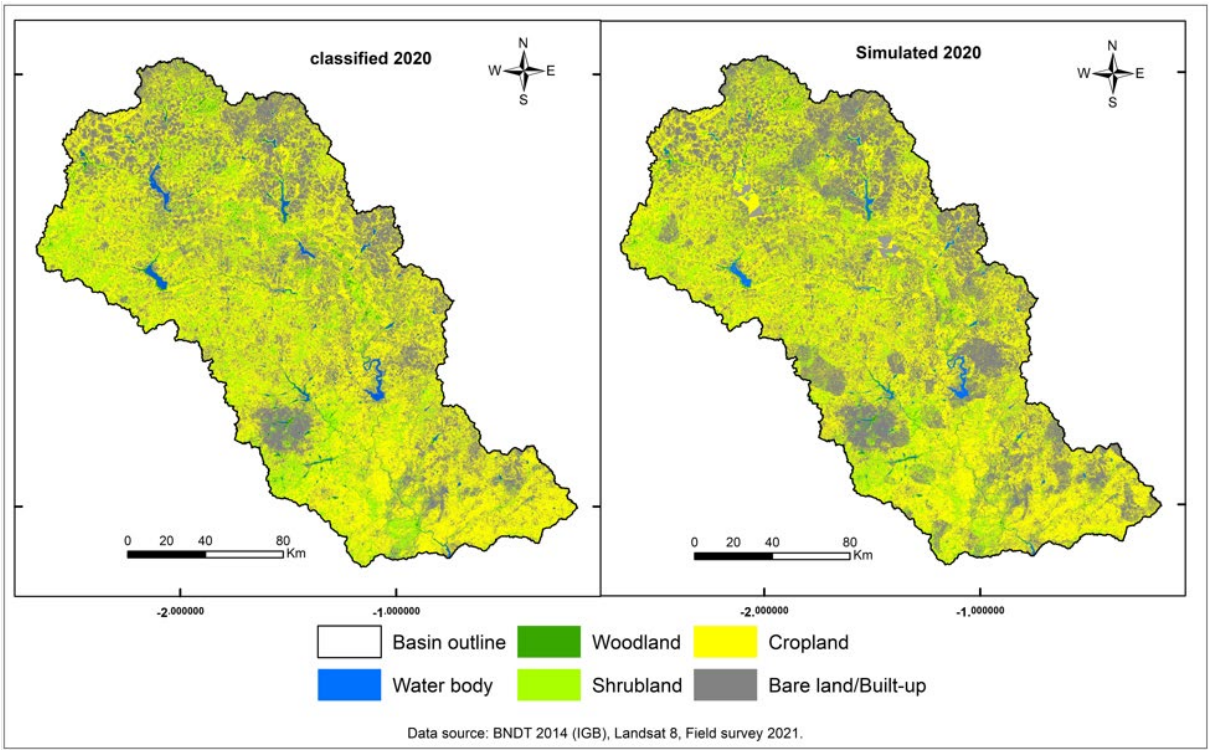

Figure 9. Actual classified (left) and simulated (right) LULC for 2020

3.8. Future LULC dynamics

The results of the LULC projection are shown in Figure 10 and Table 9. Under the BAU scenario, the basin area would be dominated in 2050 by bare land/built-up whose coverage would increase to 57.07% (Table 9), followed by cropland, shrubland, water body, and woodland with coverages of 32.95%, 7.58%, 1.35%, and 1.06%, respectively. The percentage of changes from 2020 to 2050 showed that bare land/built-up area would double while the area covered by cropland would decrease by -32% under the BAU. Natural vegetation like woodland and shrubland would decrease by -33.91% and -46.86%, respectively in 2050. On the contrary, under the afforestation scenario the basin would be mainly covered by cropland (57.76%) in 2050. Yet, woodland and shrubland would increase by 22.24% and 51.57%, respectively relative to 2020. Meanwhile the area covered by cropland would increase by 18.13% whereas bare land/built-up and water body would decrease by -39.04% and -6.16%, respectively (Table 9).

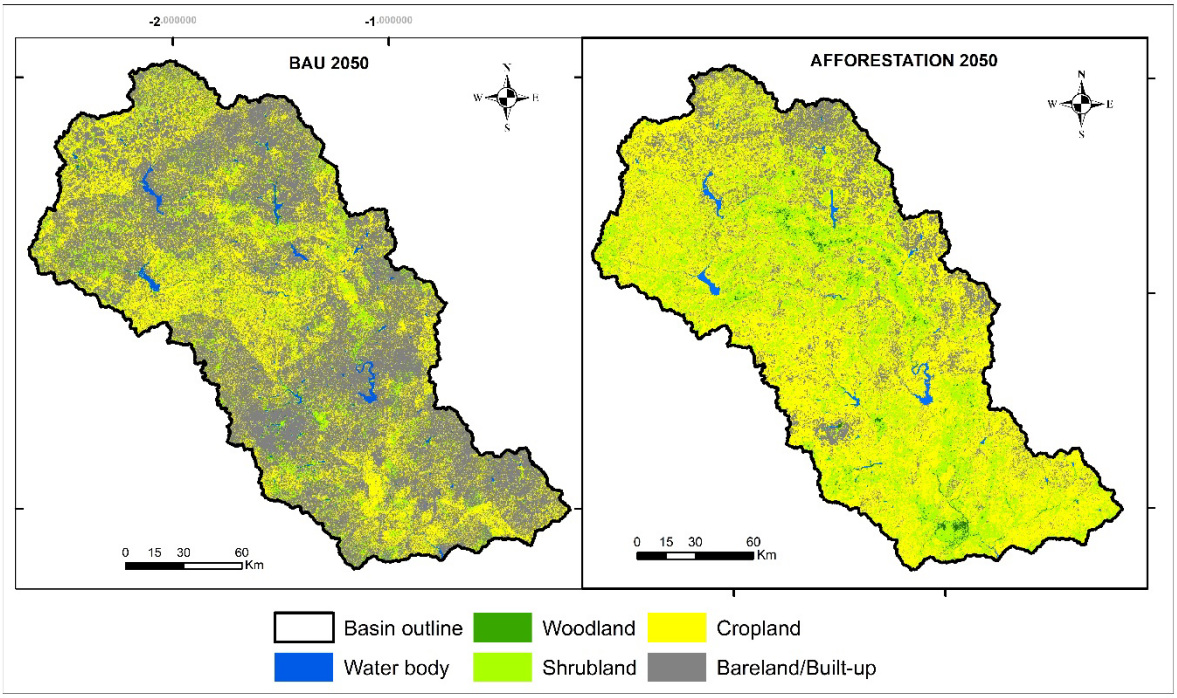

Figure 10. Projected future LULC maps for 2050 under the BAU and Afforestation scenarios

Table 9. Proportion of LULC units in 2050 under the BAU and afforestation scenarios and their percentage of changes

LULC units	Afforestation 2050		BAU 2050		Classified 2020-Afforestation 2050	Classified 2020-BAU 2050
	km^2	%	km^2	%	% Change	% Change
Water body	409.16	1.25	441	1.35	-6.16	1.15
Woodland	638.10	1.96	345	1.06	22.24	-33.91
Shrubland	7051.16	21.61	2472	7.58	51.57	-46.86
Cropland	18841.68	57.76	10749	32.95	18.13	-32.61
Bare land/Built-up	5682.90	17.42	18617	57.07	-39.04	99.71
Total	32623	100	32623	100		

4. Discussion

4.1. Classification accuracy, LCM validation, and historical LULC dynamics

The study investigated the LULC dynamic in the NRB through satellites images processing. The supervised RF classification of Landsat images on GEE gives satisfactory accuracy as Kappa > 0.75 (Fitzgerald and Lees, 1994). For the different years, the accuracy of the classification seemed to be related to the number of samples used as RF performs better when the number of samples are high (Ramezan et al. 2021). However, the low performance could also be attributed to the errors in the choice of samples. The confusion matrices show more misclassifications in samples for the year 2020 compared to 2005 and 1990, respectively. For instance, it was observed that most of confusion are between cropland and natural vegetation. This could be due to the fact that in many croplands, some selective trees are not cut because of the ecosystems services they provide. The finding is congruent with the results of Forkuor (2014) and Larbi et al. (2019) who noted a confusion between cropland and grassland classification due to the presence of grasses and trees in harvested croplands in Vea, a sub-basin of the White Volta Basin where the NRB is located.

The LCM successfully modelled the potential transitions from 1990 to 2005 with an accuracy rate of 76%. Even though Eastman (2020) suggested a threshold of 80% as acceptable performance, he also highlighted that only modelling with an accuracy lower than 75% is not effective. Yet, Rodríguez Eraso et al. (2013) agreed on a 50% threshold when using the MLP neural network to run the sub model transitions of Land use and land cover change in the Colombian Andes. Moreover, the evidence likelihood was found as most influential driver variable that explained the LULC changes from the 1990-2020 in the NRB. This was also reported in the Abbay and Nashe watersheds in Ethiopia by Hussien et al (2022) and Leta et al. (2021), respectively. Furthermore, the model showed some errors between the classified and the simulated LULC of 2020. Some LULC units were overestimated while some were underestimated. As stated by Larbi et al. (2019), these errors could be attributed to the model structure because it cannot extrapolate stationary changes from the calibration (1990-2005) to the validation period (2005-2020). These authors also emphasized the difficulty in modelling the non-linearity relationship between human and nature.

In terms of historical LULC dynamics in the NRB, the study highlighted a continuous decrease in woodland and shrubland, and a continuous increase in water bodies, cropland, and bare land/built-up from 1990 to 2020. During the last 31 years, about 50% of woodland and shrubland was converted to anthropogenic land use. This rapid conversion could be explained by the rapid population growth. Indeed, the population of the country increased from 10,312,609 to 20,487,979 inhabitants from 1996 to 2019 (INSD 2020). This population growth could result in further deforestation for farming activities. For example, a study by Ministère de l'Environnement et du Developpement Durable (2015) showed that deforestation for agriculture purposes is one of the driving factors of natural vegetation degradation in Burkina Faso. Moreover, the world forest assessment report highlighted that about 1% of forest is lost each year in the country (FAO 2010). In fact, farming in the region is still based on a familial and extensive agriculture where farms are always expanded to increase yield with little soil amendment (Jane et al. 2016; Larbi et al. 2019). Such farming techniques including slash and burn farming, aggravated by the use of non-adaptive tools and chemical fertilizers are not suitable for soil conservation (Nyamekye et al. 2018). As a result, many farms lose their fertility and become degraded. This could explain why most of the bare land/built-up net gains are from cropland conversion (Figure 3). A study by Braimoh and Vlek (2004) showed that 3% of cropland was abandoned from 1984-1992 in the Volta River Basin due to a decline in soil fertility. This finding is also evidenced by the result of the spatial trend of change. In Figures 4 and 5 for instance, where cropland replaced woodland and shrubland, there is an increase of bare land/built up area. This systematic process of transitions has been observed in other places in West Africa and South America (Barnieh et al. 2020, Rodríguez Eraso et al. 2013). In addition, many cities in Burkina Faso are experiencing increase in their areas this last decade due to a somewhat urban planning. The results of the historical LULC dynamics are congruent with those of Larbi et al. (2019), Okafor et al. (2019), Yonaba et al. (2021), and Zoungrana et al. (2015) who found the expansion of cropland, bare land and settlement areas, and a decrease in natural vegetation in the Vea, Dano, Tougou, and Southern Burkina, which are all part of the Volta River Basin where the NRB is located.

4.2. Future LULC dynamics and their implications for water resources management in the NRB

The future LULC map of 2050 in NRB was projected under the BAU and afforestation scenarios. Under the BAU scenario, a high increase in bare land/built-up and a decrease in natural vegetation and cropland from 2020 to 2050 are expected. The decrease in cropland is the result of the different transitions allowed in the Markov Chain model to compute the LULC of 2050. The results are not in agreement with many studies, which projected an increase in cropland in the future (Gupta and Sharma 2020; Larbi et al. 2019; Leta et al. 2021;). However, the findings are congruent with the results of Hussien et al. (2022) who projected a decrease in cropland (-5623.2 km^2) and an increase in settlement (1073.41 km^2) from 2021 to 2056 in the Abbay River Basin of Ethiopia. In the same country, a study by Sibanda and Ahmed (2021) projected an increase of 40% and a decrease of -18% for cropland in 2035 and 2045, respectively in the Shashe River Basin. The results of future LULC could have many impacts on water resources in the NRB. As reported by Mechal et al. (2022), the expansion of bare land could highly increase the discharge and decrease infiltration due to the higher curve number. It could also increase floods occurrence due to peak discharges (Yira et al. 2017). This situation could jeopardize the life and goods of the thousands of people who live downstream of the dams. For instance, water releases from the Bagré dam caused many deaths and economic losses in Burkina Faso and Ghana in 2009 (UNEP-GEF Volta Project 2013). The peak flows could also favour dams' siltation due to an increase in sediment transport. The high coverage of the basin by bare land/built-up could ultimately decrease low flows and affect the water yield (Balist et al. 2022).

Under the afforestation scenario, the NRB would be mostly covered by cropland (57.76%) in 2050. However, as set-up in the Markov Chain model, the area of woodland and shrubland would increase. Yet, the bare land/built-up would decrease by -39%. The statistics of LULC units in 2050 under the afforestation scenario are close to those of LULC 2005 (Tables 7 and 9). Several studies have projected a decrease in cropland to the benefit of forest in the future under the afforestation scenario (Han et al. 2015; Larbi et al. 2019). However, in this study, the increase in cropland could be attributed to bare land/built-up decrease. Indeed, the modelling assumption is set in such a way that the area covered by bare land/built-up in 2020 is mainly due to the degradation of cropland area from 2005. However, with some techniques of soil conservation such as *zaï, stone bunds, and half-moons*, some of the degraded lands could be successfully converted for agriculture purpose (Nyamekye et al. 2018). Such a policy for the designed afforestation scenario could lower the peak flows and increase the groundwater recharge through a better percolation (Tanksali and Soraganvi 2021).

5. Conclusions

This study investigated the dynamics of past and future LULC in the NRB. The method used was the RF classification in GEE, which produced acceptable maps for 1990, 2005 and 2020.The future LULC was assessed using the MLP neural network and Markov Chain of LCM. The model was successfully validated using the LULC of 2020 as reference year. The dynamic of LULC from 1990 to 2020 showed a continuous decrease in woodland and shrubland areas, a continuous increase of cropland, bare land/built-up, and water bodies. The trend of LULC units showed strong effects of human activities on land cover change in the basin. On the one hand, the future LULC map in 2050 based on the BAU scenario showed that human pressure would exacerbate the natural vegetation, with a probable decrease in cropland. On the other hand, under the afforestation scenario, the natural vegetation could increase while bare land/built-up could decrease. Some policies such as “trees planting day” which has been implemented since 2019, could help to achieve this expected increase in natural vegetation. The results of this study could ultimately be useful for the Nakambé Water Agency, a key policy maker in charge of water management in the basin. Nevertheless, the Bagré dam, a RAMSAR site located downstream of the NRB, relies on the LULC dynamics of the upstream. Therefore, other actions need to be undertaken urgently by policy makers as the success of tree planting campaigns in the country seems low.

Data availability statement

The datasets generated during and/or analysed during the current study are available from the corresponding author on reasonable request

Conflict of interest

The authors declare no conflict of interest.

References

Akinyemi FO (2021) Vegetation Trends, Drought Severity and Land Use-Land Cover Change during the Growing Season in Semi-Arid Contexts. Remote Sensing, 13(5), 836. https://doi.org/10.3390/rs13050836

Akpoti K, Antwi E, Kabo-bah A (2016) Impacts of Rainfall Variability, Land Use and Land Cover Change on Stream Flow of the Black Volta Basin, West Africa. Hydrology, 3(3), 26. https://doi.org/10.3390/hydrology3030026

Baatuuwie BN (2015) Multi-dimensional approach for evaluating land degradation in the savanna belt of the white volta basin. PhD dissertation, KNUST, Ghana.

Balist J, Malekmohammadi B, Jafari HR, Nohegar A, Geneletti D (2022) Detecting land use and climate impacts on water yield ecosystem service in arid and semi-arid areas. A study in Sirvan River Basin-Iran. Applied Water Science, 12(1), 1–14. https://doi.org/10.1007/s13201-021-01545-8

Barnieh AB, Jia L, Menenti M, Zhou J, Zeng Y (2020) Mapping Land Use Land Cover Transitions at Different Spatiotemporal Scales in West Africa. Sustainability, 12(20), 8565. https://doi.org/10.3390/su12208565

Belemsobgo U, Kafando P, Adouabou BA., Nana S, Coulibaly S, Gnoumou A (2010) Le réseau d’Aires Protégées. In : Thiombiano A., Kampmann D. (éds). Atlas de la Biodiversité de l’Afrique de l’Ouest. Tome II : Burkina Faso. Ouagadougou et Francfortt-sur-le Main, BIOTA, 592 p.

Bessah E, Raji AO, Taiwo OJ, Agodzo SK, Ololade OO, Strapasson A (2020) Hydrological responses to climate and land use changes: The paradox of regional and local climate effect in the Pra River Basin of Ghana. Journal of Hydrology: Regional Studies. 27 (23), 100654. https://doi.org/10.1016/j.ejrh.2019.100654

Bozkaya AG, Balcik FB, Goksel C, Esbah H (2015) Forecasting landcover growth using remotely sensed data: a case study of the Igneada protection area in Turkey. Environ Monit Assess. https://doi. org/ 10. 1007/ s10661- 015- 4322-z.

Braimoh AK,Vlek PLG (2004) Land-cover change analyses in the Volta Basin of Ghana. Earth Interactions, 8, p.21.

Bullock EL, Healey SP, Yang Z, Oduor P, Gorelick N, Omondi S, Ouko E, Cohen WB (2021) Three Decades of Land Cover Change in East Africa. Land, 10 (2), 150. https://doi.org/10.3390/land10020150.

Cherlet M, Hutchinson C, Reynolds J, Hill J, Sommer S, Von Maltitz G (2018) World Atlas of Desertification, Publications Office of the European Union, Luxembourg, ISBN 978-92-79-75350-3, doi:10.2760/9205, JRC111155.

CILSS (2016) Les Paysages de l'Afrique de l'Ouest : Une Fenêtre sur un Monde en Pleine Évolution. U.S. Geological Survey EROS, 47914 252nd St, Garretson, SD 57030, UNITED STATES.

Clark Labs (2020) TerrSet 2020 geospatial monitoring and modeling system. Clark Labs, Clark University, Worcester, Conway.

Dey NN, Al Rakib A, Al K, Raikwar V (2021) Geospatial modelling of changes in land use/land cover dynamics using Multi-layer perception Markov chain model in Rajshahi City, Bangladesh. Environ Chall 4:100148. https://doi.org/10.1016/j.envc.2021.100148

DGRE (2010) Etat des lieux de la gestion des ressources en eau du bassin du Nakanbé: Rapport final. https://eaunakanbe.bf/wp-content/uploads/2019/06/Rapport-etat-des-lieux-des-RE-du-Nakanbé-de-2010-Final.pdf

Dimobe K, Goetze D, Ouédraogo A, Forkuor G, Wala K, Porembski S, Thiombiano A (2017) Spatio-Temporal Dynamics in Land Use and Habitat Fragmentation within a Protected Area Dedicated to Tourism in a Sudanian Savanna of West Africa. Journal of Landscape Ecology, 10(1), 75–95. https://doi.org/10.1515/jlecol-2017-0011.

Eastman JR (2020) TerrSet geospatial monitoring and modeling system, Tutorial Version 2020.v.19.0.0. Clark University, Worcester.

FAO (2010) Rapport principal: Evaluation des ressources forestières mondiales 2010. In Etude FAO : Forêt.

Fattore C, Abate N, Faridani F, Masini N, Lasaponara R (2021) Google Earth Engine as Multi-Sensor Open-Source Tool for Supporting the Preservation of Archaeological Areas: The Case Study of Flood and Fire Mapping in Metaponto, Italy. Sensors, 21(5), 1791. https://doi.org/10.3390/s21051791

Feng D, Zhao Y, Yu L, Li C, Wang J, Clinton N, Bai Y, Belward A, Zhu Z, Gong P (2016) Circa 2014 African land-cover maps compatible with FROM-GLC and GLC2000 classification schemes based on multi-seasonal Landsat data. International Journal of Remote Sensing, 37(19), 4648–4664. https://doi.org/10.1080/01431161.2016.1218090

Findell KL, Berg A, Gentine P, Krasting JP, Lintner BR, Malyshev S, Santanello JA., Shevliakova E (2017) The impact of anthropogenic land use and land cover change on regional climate extremes. Nature Communications, 8(1), 989. https://doi.org/10.1038/s41467-017-01038-w

Fitzgerald RW, Lees BG (1994) Assessing the classification accuracy of multisource remote sensing data. Remote Sensing of Environment, 47(3), 362–368. https://doi.org/10.1016/0034-4257(94)90103-1

Floreano IX, de Moraes LAF (2021) Land use/land cover (LULC) analysis (2009–2019) with Google Earth Engine and 2030 prediction using Markov-CA in the Rondônia State, Brazil. Environmental Monitoring and Assessment, 193(4), 239. https://doi.org/10.1007/s10661-021-09016-y.

Forkuor G (2014) Agricultural Land Use Mapping in West Africa Using Multi-sensor Satellite Imagery. PhD dissertation, Julius-Maximilians-Universität, Würzburg.

Forkuor G, Hounkpatin OKL, Welp G, Thiel M (2017) High Resolution Mapping of Soil Properties Using Remote

Sensing Variables in South-Western Burkina Faso: A Comparison of Machine Learning and Multiple Linear Regression Models. PLOS ONE, 12(1), e0170478. https://doi.org/10.1371/journal.pone.0170478.

Gharaibeh A, Shaamala A, Obeidat R, Al-Kofahi S (2020) Improving land-use change modeling by integrating ANN with Cellular Automata-Markov Chain model. Heliyon. https://doi:10.1016/j.heliyon.2020.e05092. PMID: 33024869; PMCID: PMC7527583.

Girma R, Fürst C, Moges A (2022) Land use land cover change modeling by integrating artificial neural network with cellular Automata-Markov chain model in Gidabo river basin, main Ethiopian rift. Environ Chall 6:100419. https://doi.org/10.1016/j.envc.2021.100419

Gislason PO, Benediktsson JA, Sveinsson JR (2006) Random forests for land cover classification. Pattern Recognition Letters, 27(4), 294–300. https://doi.org/10.1016/j.patrec.2005.08.011

Gupta R, Sharma LK (2020) Efficacy of Spatial Land Change Modeler as a forecasting indicator for anthropogenic change dynamics over five decades: A case study of Shoolpaneshwar Wildlife Sanctuary, Gujarat, India. Ecological Indicators, 112(23), 106171. https://doi.org/10.1016/j.ecolind.2020.106171

Hackman KO, Gong P, Wang J (2017) New land-cover maps of Ghana for 2015 using Landsat 8 and three popular classifiers for biodiversity assessment. International Journal of Remote Sensing, 38(14), 4008–4021. https://doi.org/10.1080/01431161.2017.1312619

Hackman KO, Li X, Asenso-Gyambibi D, Asamoah EA, Nelson ED (2020) Analysis of geo-spatiotemporal data using machine learning algorithms and reliability enhancement for urbanization decision support. International Journal of Digital Earth. https://doi.org/10.1080/17538947.2020.1805036

Hassen G, Bantider A, Legesse A, Maimbo M, Likissa D (2021) Land use and land cover change for resilient environment and sustainable development in the Ethiopian Rift Valley Region. Ochr Sr i Zasobow Nat 32:24–41. https://doi.org/10.2478/oszn-2021-0007.

Hussien K, · Kebede A, · Mekuriaw A,· Beza SA,· Erena SH (2022) Modelling spatiotemporal trends of land use land cover dynamics in the Abbay River Basin, Ethiopia. Modeling Earth Systems and Environment. https://doi.org/10.1007/s40808-022-01487-3.

Idrissou M, Diekkrüger B, Tischbein B, Op de Hipt F, Näschen K, Poméon T, Yira Y, Ibrahim B (2022) Modeling the Impact of Climate and Land Use/Land Cover Change onWater Availability in an Inland Valley Catchment in Burkina Faso. Hydrology, 9, 12. https://doi.org/10.3390/hydrology9010012.

INSD (2020) Résultats Préliminaires du RGPH 5. http://www.insd.bf/contenu/documents_rgph5/RAPPORT_PRELIMINAIRE_RGPH_2019.pdf.

Jayne TS, Chamberlin J, Traub L, Sitko N, Muyanga M, Yeboah FK et al (2016) Africa's changing farm size distribution patterns: The rise of medium-scale farms. Agricultural Economics, 47 (S1), 197–214. https://doi.org/10.1111/agec.12308.

Karambiri H, García Galiano SG, Giraldo JD, Yacouba H, Ibrahim B, Barbier B, Polcher J (2011) Assessing the impact of climate variability and climate change on runoff in West Africa: The case of Senegal and Nakambe River basins. Atmospheric Science Letters, 12(1), 109–115. https://doi.org/10.1002/asl.317.

Kim Y, Newman G, Güneralp B (2020) A review of driving factors, scenarios, and topics in urban land change models. Land 9:1–22. https://doi.org/10.3390/LAND9080246.

Koko AF, Yue W, Abubakar GA, Hamed R, Alabsi AAN (2020) Monitoring and predicting spatio-temporal land use/land cover changes in Zaria City, Nigeria, through an integrated cellular automata and markov chain model (CA-Markov). Sustainability (Switzerland), 12(24), 1–21. https://doi.org/10.3390/su122410452

Koubodana DH, Diekkrüger B, Näschen K, Adounkpe J, Atchonouglo K (2019) Impact of the Accuracy of Land Cover Data sets on the Accuracy of Land Cover Change Scenarios in the Mono River Basin, Togo, West Africa. International Journal of Advanced Remote Sensing and GIS, 8(1), 3073–3095. https://doi.org/10.23953/cloud.ijarsg.422.

Larbi I, Forkuor G, Hountondji FCC, Agyare WA, Mama D (2019) Predictive Land Use Change under Business-As-Usual and Afforestation Scenarios in the Vea Catchment, West Africa. International Journal of Advanced Remote Sensing and GIS, 8(1), 3011–3029. https://doi.org/10.23953/cloud.ijarsg.416.

Leta MK, Demissie TA, Tränckner J (2021) Modeling and Prediction of Land Use Land Cover Change Dynamics

Based on Land Change Modeler (LCM) in Nashe Watershed, Upper Blue Nile Basin, Ethiopia. Sustainability, 13, 3740. https://doi.org/10.3390/su13073740.

Liu C, Li W, Zhu G, Zhou H, Yan H, Xue P (2020) Land Use/Land Cover Changes and Their Driving Factors in the Northeastern Tibetan Plateau Based on Geographical Detectors and Google Earth Engine: A Case Study in Gannan Prefecture. Remote Sensing; 12(19):3139. https://doi.org/10.3390/rs12193139.

Mahe G, Paturel JE, Servat E, Conway D, Dezetter A (2005) The impact of land use change on soil water holding capacity and river flow modelling in the Nakambe River, Burkina-Faso. Journal of Hydrology, 300(1–4), 33–43. https://doi.org/10.1016/j.jhydrol.2004.04.028.

Mechal A,·Takele T, Meten M, Deyassa G, Degu Y (2022) A modeling approach for evaluating the impacts of Land Use/Land Cover change for Ziway Lake Watershed hydrology in the Ethiopian Rift. Modeling Earth Systems and Environment. https://doi.org/10.1007/s40808-022-01472-w.

Mehrabi A, Khabazi M, Almodaresi SA, Nohesara M, Derakhshani R (2019) Land use changes monitoring over 30 years and prediction of future changes using multi-temporal landsat imagery and the land change modeler tools in rafsanjan city (Iran). Sustainable Development of Mountain Territories, 11(1), 26–35. https://doi.org/10.21177/1998-4502-2019-11-1-26-35.

Midekisa A, Holl F, Savory DJ, Andrade-Pacheco R, Gething PW, Bennett A, Sturrock HJW (2017) Mapping land cover change over continental Africa using Landsat and Google Earth Engine cloud computing. PLOS ONE, 12(9), e0184926. https://doi.org/10.1371/journal.pone.0184926.

Ministère de l'Environnement et du Developpement Durable (2015) Mécanisme Spécial de Dons (DGM) pour les Peuples Autochtones et les Communautés Locales. 122. https://www.iucn.org/sites/dev/files/import/downloads/cges_dgm_burkina_faso_revu_ccp_17mai15.pdf

Näschen K, Diekkrüger B, Evers M, Höllermann B, Steinbach S, Thonfeld F (2019) The Impact of Land Use/Land Cover Change (LULCC) on Water Resources in a Tropical Catchment in Tanzania under Different Climate Change Scenarios. Sustainability (Switzerland), 11(24). https://doi.org/10.3390/su11247083

Nery T, Sadler R, Solis-Aulestia M, White B, Polyakov M, Chalak M (2016) Comparing supervised algorithms in Land Use and Land Cover classification of a Landsat time-series. 2016 IEEE International Geoscience and Remote Sensing Symposium (IGARSS), 8(23), 5165–5168. https://doi.org/10.1109/IGARSS.2016.7730346

Nowak DJ, Greenfield EJ (2020) The increase of impervious cover and decrease of tree cover within urban areas globally (2012–2017). Urban Forestry & Urban Greening, 49. https://doi.org/10.1016/j.ufug.2020.126638

Nut N, Mihara M, Jeong J, Ngo B, Sigua G, Prasad PVV, Reyes MR (2021) Land Use and Land Cover Changes and Its Impact on Soil Erosion in Stung Sangkae Catchment of Cambodia. Sustainability, 13(16), 9276. https://doi.org/10.3390/su13169276

Nyamekye C, Thiel M, Schönbrodt-Stitt S, Zoungrana B, Amekudzi L (2018) Soil and Water Conservation in Burkina Faso, West Africa. Sustainability, 10(9), 3182. https://doi.org/10.3390/su10093182

Okafor GC, Annor T, Odai SN, Larbi I (2019) Land Use Landcover Change Monitoring and Projection in the Dano Catchment, Southwest Burkina Faso. International Journal of Advanced Remote Sensing and GIS, 9(1), 3185–3204. https://doi.org/10.23953/cloud.ijarsg.445.

PNUE (2004) Loss and Damage: The Role of Ecosystem Services. In Earth Interactions (Vol. 8, Issue 23). http://collections.unu.edu/view/UNU:5614.

Pontius GR (2000) Quantification error versus location error in comparison of categorical maps. Photogramm. Eng. Remote Sensing. 66, pp.1011-1016.

Prasomsup W, Piyatadsananon P, Aunphoklang W, Boonrang A (2020) Extraction Technic for Built-up Area Classification in Landsat 8 Imagery. International Journal of Environmental Science and Development, 11(1), 15–20. https://doi.org/10.18178/ijesd.2020.11.1.1219

Ramezan CA, Warner TA, Maxwell AE, Price BS (2021) Effects of Training Set Size on Supervised Machine-Learning Land-Cover Classification of Large-Area High-Resolution Remotely Sensed Data. Remote Sensing, 13(3), 368. https://doi.org/10.3390/rs13030368

Rodrguez Eraso N, Armenteras-Pascual D, Retana Alumbreros J (2013) Land use and land cover change in the Colombian Andes: dynamics and future scenarios. Journal of Land Use Science, 8:2, 154-174.

http://dx.doi.org/10.1080/1747423X.2011.650228.

Rwanga SS, Ndambuki JM (2017) Accuracy Assessment of Land Use/Land Cover Classification Using Remote Sensing and GIS. International Journal of Geosciences, 08(04), 611–622. https://doi.org/10.4236/ijg.2017.84033

Shade C, Kremer P (2019) Article predicting land use changes in philadelphia following green infrastructure policies. Land, 8(2). https://doi.org/10.3390/land8020028

Shetty S (2019) Analysis of Machine Learning Classifiers for LULC Classification on Google Earth Engine Analysis of Machine Learning Classifiers for LULC Classification on Google Earth Engine. 1–65.

Sibanda S,· Ahmed F (2021) Modelling historic and future land use/land cover changes and their impact on wetland area in Shashe sub-catchment, Zimbabwe. Modeling Earth Systems and Environment, 7:57 70. https://doi.org/10.1007/s40808-020-00963-y.

Sinha RK, Eldho TI, Subimal G (2020) Assessing the impacts of land use/land cover and climate change on surface runoff of a humid tropical river basin in Western Ghats, India. Int J River Basin Manag. https://doi.org/10.1080/15715124.2020.1809434.

Tanksali A, Soraganvi VS (2021) Modeling Earth Systems and Environment, 7:2391–2406. https://doi.org/10.1007/s40808-020-00978-5.

Thiam S, Salas EAL, Hounguè NR, Almoradie ADS, Verleysdonk S, Adounkpe JG, Komi K (2022) Modelling Land Use and Land Cover in the Transboundary Mono River Catchment of Togo and Benin Using Markov Chain and Stakeholder's Perspectives. Sustainability, 14, 4160. https://doi.org/10.3390/su14074160.

UNEP-GEF Volta Project (2013) Volta Basin Transboundary Diagnostic Analysis : http://gefvolta.iwlearn.org/project-resources/studies-reports/tda-final/regional-tda/volta-basin-tda-english.

Winkler K, Fuchs R, Rounsevell M, Herold M (2021) Global land use changes are four times greater than previously estimated. Nat Commun 12, 2501. https://doi.org/10.1038/s41467-021-22702-2.

Yang C, Wei T, Li Y (2022) Simulation and Spatio-Temporal Variation Characteristics of LULC in the Context of Urbanization Construction and Ecological Restoration in the Yellow River Basin. Sustainability. 14, 789. https://doi.org/10.3390/su14020789.

Yira Y, Diekkrüger B, Steup G, Bossa, AY (2017) Modeling land use change impacts on water resources in a tropical West African catchment (Dano, Burkina Faso). J. Hydrol., 537, pp.187-199.

Yira Y, Diekkrüger B, Steup G, Yaovi Bossa A (2017) Impact of Climate Change on Hydrological Conditions in a Tropical West African Catchment Using an Ensemble of Climate Simulations. Hydrol. Earth Syst. Sci. 21, 2143–2161.

Yonaba R, Biaou AC, Koïta M, Tazen F, Mounirou LA, Zouré CO, Queloz P, Karambiri H, Yacouba H (2021) A dynamic land use/land cover input helps in picturing the Sahelian paradox: Assessing variability and attribution of changes in surface runoff in a Sahelian watershed. Science of The Total Environment, 757(23), 143792. https://doi.org/10.1016/j.scitotenv.2020.143792.

Yu L, Liang L, Wang J, Zhao Y, Cheng Q, Hu L, Liu S, Yu L, Wang X, Zhu P, Li X, Xu Y, Li C et al (2014) Meta-discoveries from a synthesis of satellite-based land-cover mapping research. International Journal of Remote Sensing, 35(13), 4573–4588. https://doi.org/10.1080/01431161.2014.930206.

Zoungrana B, Conrad C, Amekudzi L, Thiel M, Da E, Forkuor G, Löw F (2015) Multi-Temporal Landsat Images and Ancillary Data for Land Use/Cover Change (LULCC) Detection in the Southwest of Burkina Faso, West Africa. Remote Sensing, 7(9), 12076–12102. https://doi.org/10.3390/rs70912076.